Lattice thermal conductivity of group-IV and III–V semiconductor alloys

Sadao Adachi[a)]
Department of Electronic Engineering, Faculty of Engineering, Gunma University, Kiryu-shi, Gunma 376-8515, Japan

(Received 17 June 2007; accepted 23 July 2007; published online 17 September 2007)

The room-temperature thermal conductivity of semiconductor alloys is analyzed using a simplified model of the alloy-disorder scattering. Good agreement is achieved between the present model and published experimental data on various group-IV and III−V semiconductor alloys. A complete set of alloy-disorder parameters are estimated, which makes it possible to calculate the lattice thermal conductivity for optional composition of III−V semiconductor alloys, including III−N alloys. An ordering effect is also examined for the explanation of some intermetallic and semiconductor compounds like CuAu and SiC. © *2007 American Institute of Physics*. [DOI: 10.1063/1.2779259]

I. INTRODUCTION

Knowledge of the thermal conductivity of semiconductors forms an important part in the design of power-dissipating devices, such as diodes, transistors, and optoelectronic devices (lasers, light-emitting diodes, etc.). The thermal conductivity is also necessary in calculating the figure of merit for thermoelectric devices (Seebeck and Peltier devices).

Abeles[1] proposed a phenomenological model to analyze the lattice thermal conductivity of semiconductor alloys at high temperatures. He analyzed the experimental data of several semiconductor alloys in a satisfactory manner in terms of the three-phonon and point-defect scatterings. Abeles's model, however, requires various material parameters and adjustable constants to achieve the best fit between calculation and experiment. Therefore, Adachi[2] simplified his model and used to estimate the lattice thermal conductivity as a function of alloy composition for $Ga_xIn_{1-x}P_yAs_{1-y}$ lattice matched to InP. Abeles's model has also been extended by Nakwaski.[3]

The purpose of this article is to further study the room-temperature lattice thermal conductivity of semiconductor alloys, including III−N alloys. After the publication of Adachi,[2] there have been an accumulation of the experimental data on various semiconductor alloys. Despite of study, only recently has III−N semiconductors changed from a research curiosity to commercially very important semiconductors. No III−N semiconductors were discussed in the previous article.[2] In this article, a complete set of alloy-disorder parameters will be determined for the calculation of the lattice thermal conductivity of III−V semiconductor alloys, including III−N ternary and quaternary alloys, with optional compositions.

II. FUNDAMENTAL ASPECT

An exact calculation of the lattice thermal conductivity K is possible, in principle, but lack of knowledge of various materials (e.g., anharmonic forces and lattice vibration spectra) and the difficulty of obtaining exact solution of phonon-phonon interactions are formidable barriers. In the case of semiconductor alloys, an additional contribution, which is the result of a random distribution of constituent atoms in sublattice sites, should be taken into consideration. A phenomenological model of the lattice thermal conductivity for semiconductor alloys was first proposed by Abeles.[1] He did calculations using an analysis of the lattice thermal conductivity that was reasonably successful for semiconductor alloys. His model starts from three kinds of relaxation times: $\tau_N^{-1}=B_1\omega^2$ (three-phonon normal process), $\tau_U^{-1}=B_2\omega^2$ (three-phonon Umklapp process), and $\tau_D^{-1}=A\Gamma\omega^2$ (strain and mass point defects), where ω is the phonon frequency, B_1, B_2, and A are constants independent of ω, and Γ is the disorder parameter depending on the masses and radii of the constituent atoms.

Abele's model was used by Adachi[2] and Nakwaski[3] for several III−V semiconductor alloys. Adachi[2] showed that for $A_xB_{1-x}C$ alloy the simple expression

$$W(x)=xW_{AC}+(1-x)W_{BC}+x(1-x)C_{A-B} \tag{1}$$

is essentially the same as Eq. (22) in Ref. 1, where W_{AC} and W_{BC} are the binary thermal resistivities and C_{A-B} is a contribution arising from the lattice disorder (Γ) due to the random distribution of A and B atoms in the cation (or anion) sublattice sites. Equation (1) is known as Norbury's rule[4,5] and can be readily converted to the lattice thermal conductivity K,

$$K(x)=\frac{1}{W(x)}=\frac{1}{xW_{AC}+(1-x)W_{BC}+x(1-x)C_{A-B}}. \tag{2}$$

In an $A_xB_{1-x}C_yD_{1-y}$ quaternary alloy, not only should the $A-B$ disorder due to the random distribution of the A and B atoms in the cation sublattice and the $C-D$ disorder due to the random distribution of the C and D atoms in the anionic sublattice be taken into consideration, but also the fact that both the cation and anion sublattices are disordered as well.[3] Neglecting the cation-anion interaction effect, we obtain

a)Electronic mail: adachi@el.gunma-u.ac.jp

$$K(x,y)=\frac{1}{W(x,y)}=\frac{1}{xyW_{AC}+x(1-y)W_{AD}+(1-x)yW_{BC}+(1-x)(1-y)W_{BD}+x(1-x)C_{A-B}+y(1-y)C_{C-D}}. \tag{3}$$

In doped semiconductors, the total thermal conductivity can be given by the sum of the lattice and electronic contributions. In a metal, the electronic thermal conductivity K and electrical conductivity σ at temperature T are related by the Wiedemann–Franz law

$$K=LT\sigma, \tag{4}$$

or, equivalently

$$\rho=LTW, \tag{5}$$

where L is the Lorenz number and ρ is the electrical resistivity.

Cu-Au alloy is among the best studied of all metallic alloy systems. The most interesting feature of this alloy is that CuAu (x=0.5) and Cu_3Au (x=0.75) can be obtained in either ordered or disordered form. Let us show in Fig. 1 the electrical (ρ) and thermal resistivities (W) as a function of composition x for Cu_xAu_{1-x} alloy. The solid circles represent the experimental data obtained from ordered alloys (CuAu and Cu_3Au), while the open circles represent the data obtained from disordered alloys. These data were gathered from various sources (see, e.g., Ref. 6). The dashed lines are calculated from Eq. (1) with (a) $C_{\text{Cu-Au}}$=60 $\mu\Omega$ cm and (b) $C_{\text{Cu-Au}}$=8.15 cm K/W. It is evident from Fig. 1 that the values of ρ and W for the intermetallic compounds CuAu and Cu_3Au are extremely smaller than those estimated from Eq. (1). It is, thus, concluded that the ordering in metallic alloy decreases the electrical and thermal resistivities, irrespective of crystal structure (CuAu=$L1_0$ or Cu_3Au=$L1_2$).

In semiconductor alloys, the phenomenon of spontaneous ordering has been observed to occur spontaneously during epitaxial growth of certain semiconductor alloys.[7] Kuan *et al.*[8] first observed an ordered phase (CuAu-I type) in III–V semiconductor alloy which was an AlGaAs epilayer grown on GaAs (100) substrate at 600–800 °C by metalorganic chemical vapor deposition (MOCVD). Since the first finding of CuPt-type ordering in SiGe alloy,[9] this type of ordering (CuPt-B) has also been reported for many III–V semiconductors, such as AlInP, GaInP, AlInAs, and GaInAs.[7] New types of ordering, CuPt-A and TP-A, have also been observed in AlInP and AlInAs alloys.

Figure 2 shows the inverse hole mobility μ_h^{-1} and thermal resistivity W against composition x for $Al_xGa_{1-x}As$ ternary alloy. The hole mobility data plotted are gathered from many sources, while the thermal resistivities are taken from Afromowitz[10] and Pichardo *et al.*[11] It should be noted that the hole mobility μ_h is related to the electrical resistivity ρ by the relation $\rho=(ep\mu h)^{-1}$, where e is the elementally charge and p is the hole concentration. The dashed lines in Figs. 2(a) and 2(b) are calculated from Eq. (1) with $C_{\text{Al-Ga}}$ =0.013 V s/cm^2 and $C_{\text{Al-Ga}}$=32 cm K/W, respectively.

The electrons in metallic and semiconductor alloys see potential fluctuations as a result of the compositional disorder. This effect produces a peculiar scattering mechanism, namely, alloy scattering. The alloy-scattering or alloy-disorder term C_{A-B} determined in Fig. 2(a) can be expressed as[12]

$$C_{A-B}=\left[\frac{\sqrt{2\pi}}{3}\frac{e\hbar^4N_{\text{dl}}}{(kT)^{1/2}(m_h)^{5/2}(\Delta U_h)^2}\right]^{-1}, \tag{6}$$

where N_{dl} is the density of alloy sites, m_h is the hole effective mass, and ΔU_h is the alloy scattering potential. Because of

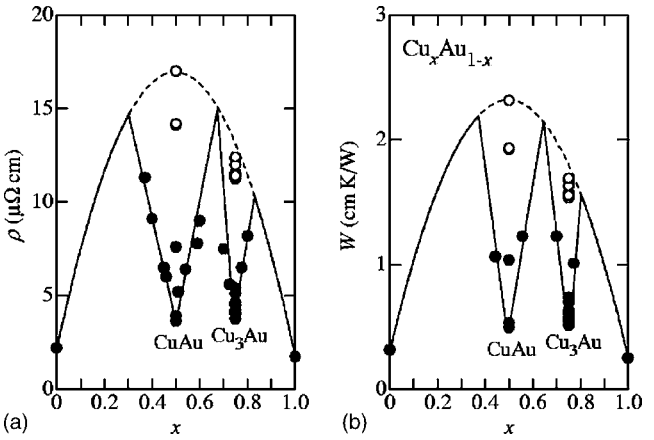

FIG. 1. (a) Electrical ρ and (b) thermal resistivities W as a function of alloy composition x for Cu_xAu_{1-x}. The experimental data are gathered from various sources. The solid circles represent the experimental data obtained from ordered alloys (CuAu and Cu_3Au), while the open circles represent the data taken from disordered alloys. The dashed lines in (a) and (b) are calculated from Eq. (1) with $C_{\text{Cu-Au}}$=60 $\mu\Omega$ cm and $C_{\text{Cu-Au}}$=8.15 cm K/W, respectively.

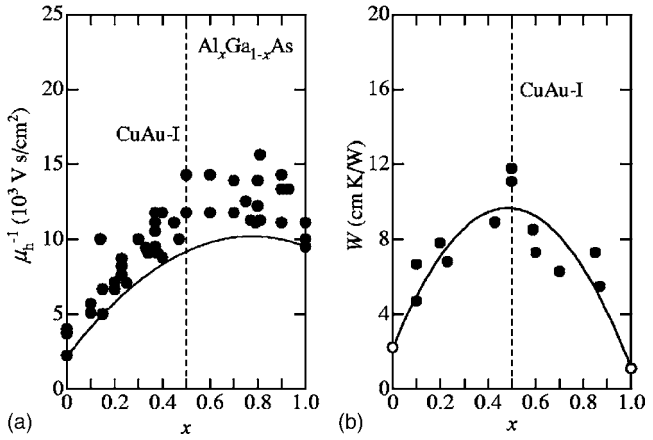

FIG. 2. (a) Inverse hole mobility μ_h^{-1} and (b) thermal resistivity W as a function of alloy composition x for $Al_xGa_{1-x}As$ ternary. The hole mobility data are gathered from many sources, while the thermal resistivities are taken from Afromowitz[10] and Pichardo *et al.*[11] The open circles in (b) represent the experimental data of the end point materials listed in Table I. The dashed lines in (a) and (b) are calculated from Eq. (1) with $C_{\text{Al-Ga}}$ =0.013 V s/cm^2 and $C_{\text{Al-Ga}}$=32 cm K/W, respectively.

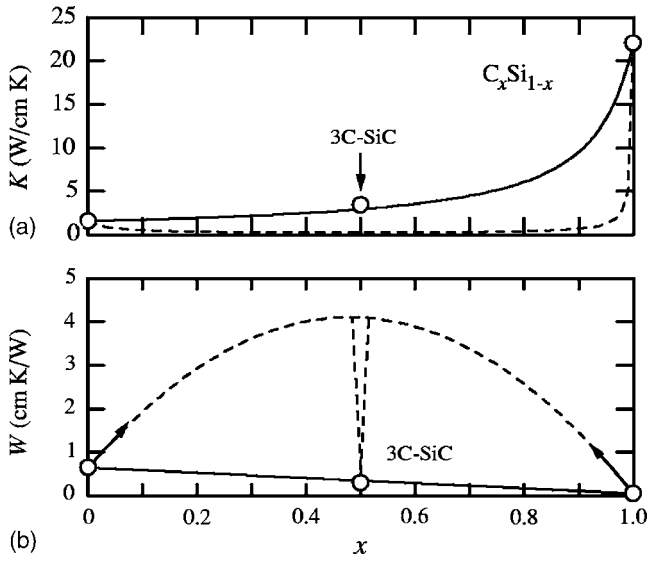

FIG. 3. (a) Thermal conductivity K and (b) resistivity W vs composition x for C_xSi_{1-x} binary alloy. The experimental data of C (diamond), Si, and 3C-SiC (x=0.5) are taken from Adachi (see also Table I).[14] The solid lines are calculated from Eqs. (1) and (2) without taking into account the alloy-disorder contribution ($C_{C\text{-}Si}$=0 cm K/W), while the dashed lines are calculated with assuming $C_{C\text{-}Si}$=15 cm K/W.

the only strong disorder effect seen in Fig. 2, we consider this effect, but not an ordering effect, in the present analysis except for C_xSi_{1-x} (SiC).

III. ANALYSIS

A. Group-IV semiconductor alloy

There has been no experimental or theoretical work on the thermal conductivity of C_xSi_{1-x} alloy. This is because of the low solubility of C into Si ($\sim 6\times 10^{-6}$). A few atomic percent of C incorporated into substitutional lattice sites of Si has been achieved only using growth techniques far from thermodynamic equilibrium (e.g., molecular beam epitaxy and MOCVD).[13] In Fig. 3, we therefore plot only the experimentally available K and W values of 3C-SiC (x=0.5),[14] together with those of the end point constituents C (diamond) and Si. Note that C and Si crystallize in the diamond structure, while 3C-SiC crystallizes in the zinc blende structure. It is, therefore, recognized that 3C-SiC is an ordered form of C_xSi_{1-x} alloy (x=0.5), or more straightly, it is a compound, not an alloy.

The solid lines in Fig. 3 are calculated from Eqs. (1) and (2) without taking into account the alloy-disorder contribution ($C_{C\text{-}Si}$=0 cm K/W), while the dashed lines are calculated with assuming $C_{C\text{-}Si}$=15 cm K/W. The C and Si values used in the calculation are listed in Table I. It is understood from Fig. 3 that the thermal conductivity and resistivity of 3C-SiC are well interpreted by the linear interpolation scheme between the end point constituents (C_{A-B}=0 cm K/W). It is also expected from Fig. 3 that substitution of C (Si) atoms into Si (C) lattice sites greatly decreases its K value due to increased disorder scattering. Similarly, not only a large decrease in doped Si,[15,16] but also an increase in isotopically enriched C (Refs. 17 and 19) and Si (Refs. 16 and 20) have been reported.

TABLE I. Thermal conductivity K and resistivity W for some group-IV elemental and III−V binary semiconductors (Ref. 14), together with the disorder-scattering parameter $C_{\alpha-\beta}$.

Material	K (W/cm K)	W (cm K/W)	$C_{\alpha-\beta}$ (cm K/W)
C (diamond)	22	0.045	$C_{Si\text{-}Ge}$=50
Si	1.56	0.64	$C_{Al\text{-}Ga}$=32
Ge	0.6	1.67	$C_{Al\text{-}In}$=15 [a]
AlN	3.19	0.31	$C_{Ga\text{-}In}$=72
AlP	0.90	1.1	$C_{N\text{-}P}$=36 [a]
AlAs	0.91	1.10	$C_{N\text{-}As}$=12 [a]
AlSb	0.57	1.75	$C_{N\text{-}Sb}$=10 [a]
GaN	1.95	0.51	$C_{P\text{-}As}$=25
GaP	0.77	1.30	$C_{P\text{-}Sb}$=16 [a]
GaAs	0.45	2.22	$C_{As\text{-}Sb}$=91
GaSb	0.36	2.78	
InN	0.45	2.22	
InP	0.68	1.47	
InAs	0.30	3.3	
InSb	0.175	5.71	

[a]Estimated from Eq. (11).

Systematic work on thermal conductivity of Si_xGe_{1-x} binary alloy was performed by Dismukes *et al.*[21] We plot in Fig. 4 their obtained K and W versus x for Si_xGe_{1-x} alloy. The solid lines represent the calculated results of Eqs. (1) and (2) with $C_{Si\text{-}Ge}$=50 cm K/W. The experimental data show that the thermal resistivity markedly increases with alloying. The W value at $x\sim 0.5$ is about 20 and 8 times as large as those of Si and Ge. Such a feature was motivated by desire to obtain increased performance for thermoelectric power conversion since the figure of merit for such device applications varies proportionally to W. One method of achieving high W value is by the use of the fine grain SiGe technique, in which a thermal conductivity decrease of up to

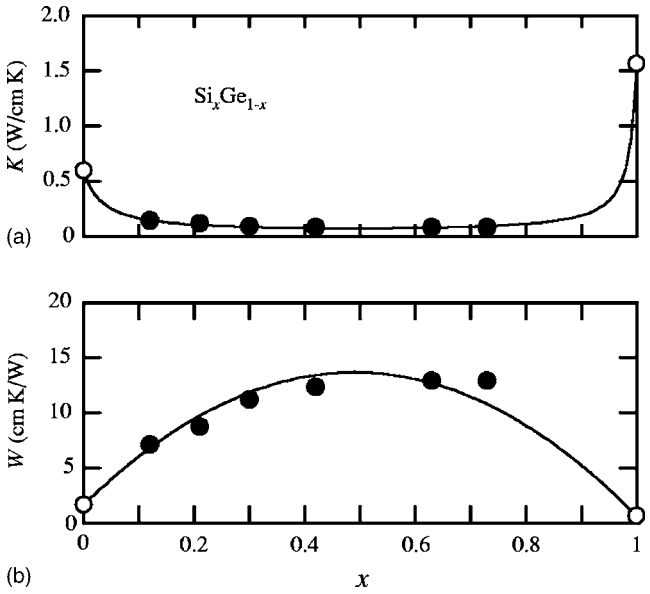

FIG. 4. (a) Thermal conductivity K and (b) resistivity W vs composition x for Si_xGe_{1-x} alloy. The experimental data are taken from Dismukes *et al.*[21] The open circles represent the experimental data of the end point materials listed in Table I. The solid lines are obtained from Eqs. (1) and (2) with $C_{Si\text{-}Ge}$=50 cm K/W.

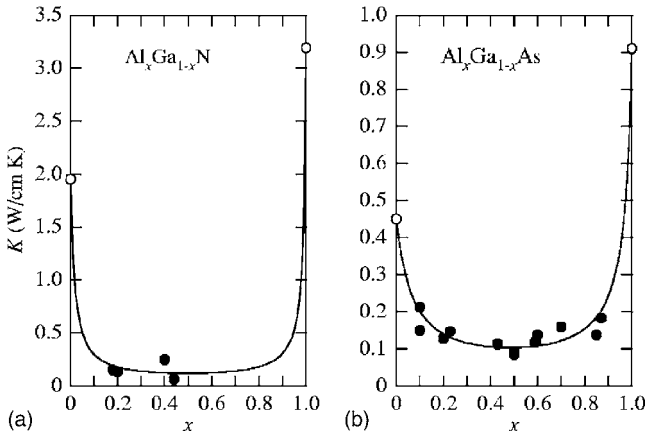

FIG. 5. Thermal conductivity K vs composition x for (Al, Ga)-based III−V ternary alloys: (a) $Al_xGa_{1-x}N$ and (b) $Al_xGa_{1-x}As$. The experimental data in (a) are taken from Daly *et al.*[23] and Liu and Balandin[24] and those in (b) are from Afromowitz[10] and Pichardo *et al.*[11] The open circles represent the experimental data of the end point binary materials listed in Table I. The solid lines are obtained from Eq. (2) with $C_{\text{Al-Ga}}=32$ cm K/W.

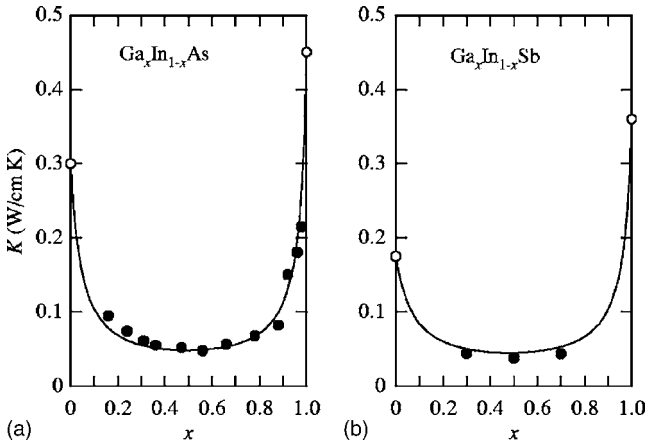

FIG. 6. Thermal conductivity K vs composition x for (Ga, In)-based III−V ternary alloys: (a) $Ga_xIn_{1-x}As$ and (b) $Ga_xIn_{1-x}Sb$. The experimental data in (a) are taken from Abrahams *et al.*[26] and Arasly *et al.*[27] and those in (b) are from Magomedov *et al.*[28] The open circles represent the experimental data of the end point binary materials listed in Table I. The solid lines are obtained from Eq. (2) with $C_{\text{Ga-In}}=72$ cm K/W.

50% was attained by increasing grain boundary scattering of phonons.[22] It is clear from Fig. 4 that the present model [Eqs. (1) and (2)] shows an excellent agreement with the experimental data.

B. III−V ternary alloy

Figure 5 shows the thermal conductivity K versus composition x for (Al, Ga)-based III−V ternary alloys: (a) $Al_xGa_{1-x}N$ and (b) $Al_xGa_{1-x}As$. The experimental data are taken for $Al_xGa_{1-x}N$ from Daly *et al.*[23] and Liu and Balandin[24] and for $Al_xGa_{1-x}As$ from Afromowitz[10] and Pichardo *et al.*[11] The solid lines represent the calculated results of Eq. (2). The III−V binary data used in the calculation are taken from Table I. The reduction in K from the binary value is much larger in the $Al_xGa_{1-x}N$ alloy than in the $Al_xGa_{1-x}As$ alloy. However, these (Al, Ga)-based ternary alloys have the same disorder parameter value $C_{\text{Al-Ga}}=32$ cm K/W (solid lines). It is also reported[23] that the polycrystalline GaN has a thermal conductivity K, which is more than an order of magnitude lower than that of the bulk GaN.

It should be noted that the thermal conductivity K (or thermal resistivity $W=K^{-1}$) is a quantity given by a second-rank symmetric tensor.[14] The wurtzite-type III−N semiconductors, AlN, GaN, and InN, thus have two tensor components, $K_\perp$ and $K_\parallel$. However, the difference between $K_\perp$ and $K_\parallel$ usually appears to be less than the experimental uncertainty at room temperature.[25]

Figure 6 shows the thermal conductivity K versus composition x for (Ga, In)-based III−V ternary alloys: (a) $Ga_xIn_{1-x}As$ and (b) $Ga_xIn_{1-x}Sb$. The experimental data are taken for $Ga_xIn_{1-x}As$ from Abrahams *et al.*[26] and Arasly *et al.*[27] and for $Ga_xIn_{1-x}Sb$ from Magomedov *et al.*[28] The solid lines represent the calculated results of Eq. (2) with $C_{\text{Ga-In}}=72$ cm K/W.

It is well known that dilute alloying of GaAs with InAs is a very effective technique for reducing the dislocation density of semi-insulating crystals grown by the liquid-encapsulated Czochralski method. Ohmer *et al.*[29] studied the effect of small addition of InAs on the thermal properties of GaAs. They obtained that for $x=0.005$ the thermal conductivity is reduced to 50% of the GaAs value. This region is in accordance with theory if the size difference is considered and combined coherently with the mass difference.[30]

The thermal conductivity K and resistivity W versus composition x for $AlAs_xSb_{1-x}$ ternary alloy are shown in Figs. 7(a) and 7(b), respectively. The experimental data are taken from Borca-Tasciuc *et al.*[31] The solid lines are calculated from Eqs. (1) and (2) with $C_{\text{As-Sb}}=91$ cm K/W. The agreement between the calculation and experiment is found to be very good.

The lattice thermal conductivity K versus x plots for (P, As)-based III−V ternary alloys GaP_xAs_{1-x} and InP_xAs_{1-x} are shown in Figs. 8(a) and 8(b), respectively. The experimental

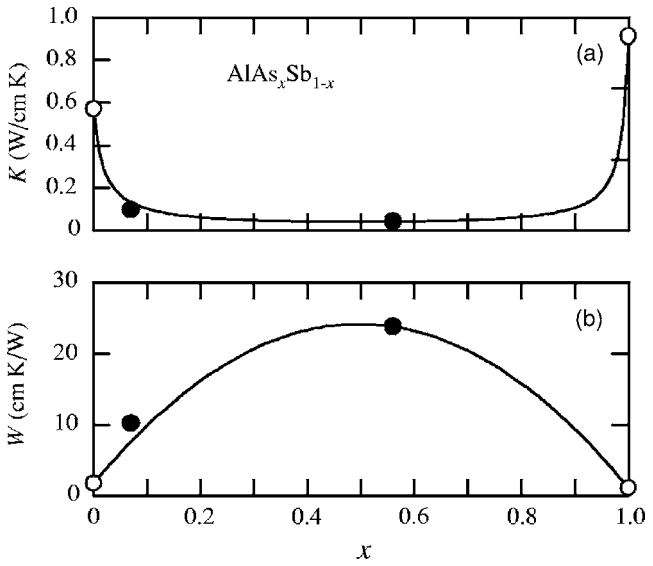

FIG. 7. (a) Thermal conductivity K and (b) resistivity W vs composition x for $AlAs_xSb_{1-x}$ ternary alloy. The experimental data are taken from Borca-Tasciuc *et al.*[31] The open circles represent the experimental data of the end point binary materials listed in Table I. The solid lines are obtained from Eqs. (1) and (2) with $C_{\text{As-Sb}}=91$ cm K/W.

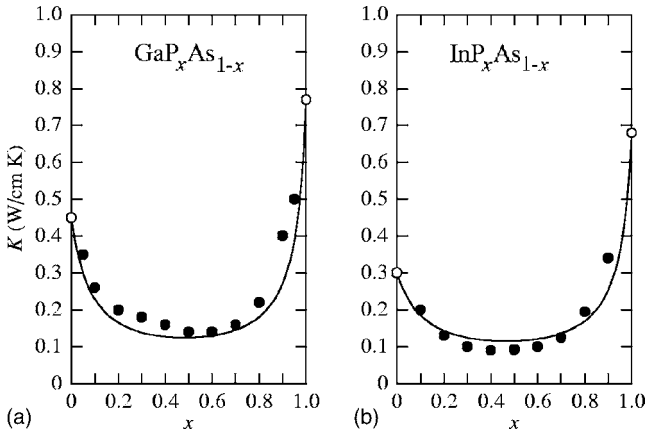

FIG. 8. Thermal conductivity K vs composition x for (P, As)-based III−V ternary alloys: (a) GaP_xAs_{1-x} and (b) InP_xAs_{1-x}. The experimental data in (a) are taken from Carlson *et al.*[32] and Maycock[33] and those in (b) are from Maycock[33] and Bowers *et al.*[34] The open circles represent the experimental data of the end point binary materials listed in Table I. The solid lines are obtained from Eq. (2) with $C_{\text{P-As}}=25$ cm K/W.

data are taken for GaP_xAs_{1-x} from Carlson *et al.*[32] and Maycock[33] and for InP_xAs_{1-x} from Maycock[33] and Bowers *et al.*[34] The solid lines represent the calculated results of Eq. (2) with $C_{\text{P-As}}=25$ cm K/W. The fit-determined disorder parameter is $C_{\text{P-As}}=25$ cm K/W, which is comparable to $C_{\text{Al-Ga}}=32$ cm K/W but much smaller than $C_{\text{Ga-In}}=72$ cm K/W and $C_{\text{As-Sb}}=91$ cm K/W.

C. III−V quaternary alloy

After the publication of Adachi,[2] some authors reported the experimental thermal conductivity of III−V semiconductor quaternary alloys. We show in Fig. 9 the results of these measurements. The experimental data are taken for (a) $Al_xGa_{1-x}As_ySb_{1-y}$ lattice matched to GaSb from Borca-Tasciuc *et al.*[31] and Both *et al.*,[35] for (b) $Ga_xIn_{1-x}P_yAs_{1-y}$ lattice matched to InP from Both *et al.*,[36] and for (c) $Ga_xIn_{1-x}As_ySb_{1-y}$ lattice matched to GaSb from Both *et al.*[35]

The theoretical curves in Fig. 9 are obtained from Eq. (3) with (a) $C_{\text{Al-Ga}}=32$ cm K/W and $C_{\text{As-Sb}}=91$ cm K/W, (b) $C_{\text{Ga-In}}=72$ cm K/W and $C_{\text{P-As}}=25$ cm K/W, and (c) $C_{\text{Ga-In}}=72$ cm K/W and $C_{\text{As-Sb}}=91$ cm K/W. All these disorder parameters $C_{\alpha-\beta}$'s are determined from the analysis of the III−V ternary data. The lattice-matching relations between the compositions x and y can be expressed as

$$y=\frac{0.0396x}{0.4426+0.0315x}\cong 0.084x \quad (0\le x\le 1.0,\ 0\le y\le 0.084), \tag{7}$$

for $Al_xGa_{1-x}As_ySb_{1-y}$/GaSb,

$$x=\frac{0.1893-0.1893y}{0.4050+0.0132y}\cong 0.47-0.47y \quad (0\le x\le 0.47,\ 0\le y\le 1.0), \tag{8}$$

for $Ga_xIn_{1-x}P_yAs_{1-y}$/InP, and

$$y=\frac{0.3834-0.3834x}{0.4211+0.0216x}\cong 0.91-0.91x \quad (0\le x\le 1.0,\ 0\le y\le 0.91), \tag{9}$$

for $Ga_xIn_{1-x}As_ySb_{1-y}$/GaSb.

The agreement between the experimental data and our calculation in Figs. 9(a) and 9(b) is very good and represents the successful explanation of the compositional variation of the lattice thermal conductivity in the alloys. It should be noted, however, that our calculation in Fig. 9(c) produces considerably lower K value than the experimental one. The input of very small $C_{\alpha-\beta}$ values into Eq. (3) improves the fit of the quaternary data very well; however, the end point ternary K value ($InAs_{0.91}Sb_{0.09}$, $x=0$) becomes very large and the binary K value (GaSb, $x=1.0$) very small, compared with the generally accepted values. The dashed line in Fig. 9(c) represents an example of this calculation. Putting $C_{\text{Ga-In}}=10$ cm K/W and $C_{\text{As-Sb}}=20$ cm K/W into Eq. (3), we obtain $K=0.30$ W/cm K for $x=0$ ($InAs_{0.91}Sb_{0.09}$) and 0.25 W/cm K for $x=1.0$ (GaSb), which are far from the generally accepted values.

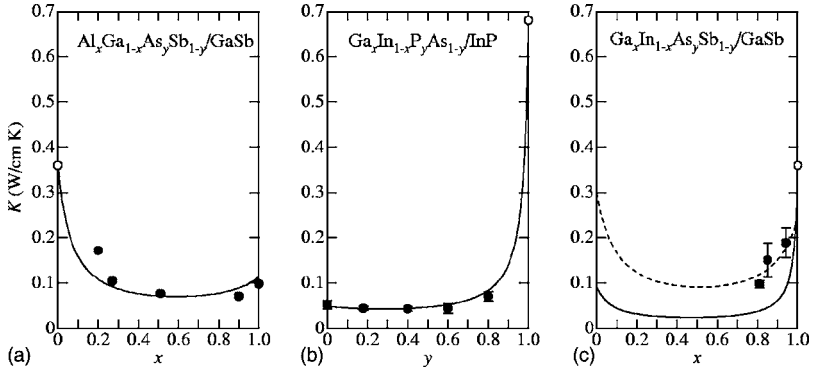

FIG. 9. Thermal conductivity K vs composition x or y for III−V quaternary alloys: (a) $Al_xGa_{1-x}As_ySb_{1-y}$/GaSb, (b) $Ga_xIn_{1-x}P_yAs_{1-y}$/InP, and (c) $Ga_xIn_{1-x}As_ySb_{1-y}$/GaSb. The experimental data are taken for $Al_xGa_{1-x}As_ySb_{1-y}$/GaSb from Borca-Tasciuc *et al.*[31] and Both *et al.*,[35] for $Ga_xIn_{1-x}P_yAs_{1-y}$/InP from Both *et al.*,[36] and for $Ga_xIn_{1-x}As_ySb_{1-y}$/GaSb from Both *et al.*[35] The open circles represent the experimental data of the end point binary materials listed in Table I (GaSb and InP). The solid lines are calculated from Eq. (3) with (a) $C_{\text{Al-Ga}}=32$ cm K/W and $C_{\text{As-Sb}}=91$ cm K/W, (b) $C_{\text{Ga-In}}=72$ cm K/W and $C_{\text{P-As}}=25$ cm K/W, and (c) $C_{\text{Ga-In}}=72$ cm K/W and $C_{\text{As-Sb}}=91$ cm K/W. The dashed line in (c) represents the calculated result of Eq. (3) by introducing the very small disorder parameters $C_{\text{Ga-In}}=10$ cm K/W and $C_{\text{As-Sb}}=20$ cm K/W.

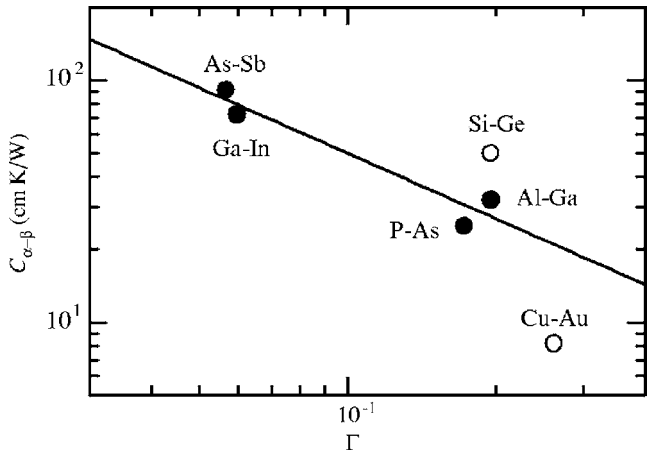

FIG. 10. $C_{\alpha-\beta}$ vs Γ determined for some group-IV binary and III−V ternary alloys and metallic Cu-Au alloy. The solid line represents the least-squares fit of the III−V ternary data using Eq. (11).

IV. ESTIMATION OF *K* VALUE

If the end point K values and $C_{\alpha-\beta}$'s are available, one can easily calculate from Eq. (2) or Eq. (3) the lattice thermal conductivity and its dependence on alloy composition. In the limit of weak scattering, the disorder parameter Γ in Ref. 1 can be simply written as

$$\Gamma = \sum_i c_i \left(\frac{M_i - \bar{M}}{\bar{M}} \right)^2, \tag{10}$$

where c_i is the fractional concentration of the ith species, M_i is the atomic mass of the ith species, and $\bar{M}$ is the average atomic mass.

We plot in Fig. 10 our obtained $C_{\alpha-\beta}$ versus Γ. It is found that $C_{\alpha-\beta}$ decreases with increasing Γ. The solid line represents the least-squares fit of the III−V ternary values given by ($C_{\alpha-\beta}$ in cm K/W),

$$C_{\alpha-\beta} = \left(\frac{\Gamma}{7.7} \right)^{-0.90}. \tag{11}$$

Using this expression, we can estimate the unknown $C_{\alpha-\beta}$ value. For example, Γ of the cationic disorder system i =(Al,In) is 0.384. Introducing this Γ value into Eq. (11), we obtain $C_{\text{Al-In}}$=15 cm K/W.

Figure 11 shows the lattice thermal conductivity as a function of alloy composition x for (a) $Ga_xIn_{1-x}N$, (b) $Ga_xIn_{1-x}P$, and (c) $GaAs_xSb_{1-x}$. No experimental data are available for these alloys. The solid lines are calculated from Eq. (2) with $C_{\text{Ga-In}}$=72 cm K/W [(a) and (b)] and $C_{\text{As-Sb}}$ =95 cm K/W (c). As expected, the calculated K values markedly decrease with alloying and exhibit a maximum at $x \sim 0.5$. It should be noted that the value of W_{InN} =2.22 cm K/W used in the calculation of Fig. 11(a) corresponds to that for InN ceramics, not the bulk crystalline value. The dashed line in Fig. 11(a) shows the calculated result of Eq. (2) using a properly chosen value of W_{InN} =0.5 cm K/W, instead of the ceramics value W_{InN} =2.22 cm K/W (solid line). The small W_{InN} effect is remarkable only in the limited region $x < 0.2$.

In an $A_xB_yC_zD$ ($AB_xC_yD_z$) quaternary alloy, the lattice thermal conductivity K can be written as

$$K(x,y,z) = \frac{1}{W(x,y,z)} = \frac{1}{xW_{AD} + yW_{BD} + zW_{CD} + C_{A-B}xy + C_{A-C}xz + C_{B-C}yz}, \tag{12}$$

with

$$x + y + z = 1 \quad \text{or} \quad z = 1 - x - y. \tag{13}$$

Since the thermal conductivity or resistivity in Eq. (12) is specified in terms of the alloy compositions x, y, and z only, we can easily calculate K or W of quaternary alloy with arbitrary composition. For example, the thermal conductivity of $Al_xGa_yIn_{1-x-y}N$ can be estimated from (K in W/cm K),

$$K_{\text{AlGaInN}}(x,y,z) = \frac{1}{3.19x + 1.95y + 0.45z + 32xy + 15xz + 72yz}. \tag{14}$$

Similarly, we can estimate the K values of $Al_xGa_yIn_{1-x-y}P$ lattice-matched to GaAs and $Al_xGa_yIn_{1-x-y}As$ lattice-matched to InP, as shown in Fig. 12. The disorder parameters $C_{\alpha-\beta}$ used are taken from Table I. The lattice-matching relations between x and y for these quaternary alloys are

$$y = 0.5158 - 0.9696x \quad (0 \le x \le 0.53, 0 \le y \le 0.52), \tag{15}$$

for $Al_xGa_yIn_{1-x-y}P/GaAs$, and

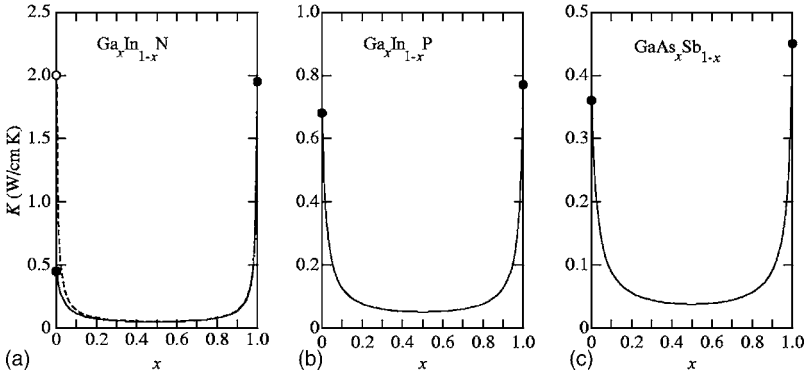

FIG. 11. Thermal conductivity K vs composition x for some III−V ternary alloys: (a) $Ga_xIn_{1-x}N$, (b) $Ga_xIn_{1-x}P$, and (c) $GaAs_xSb_{1-x}$. These estimated values are calculated from Eq. (2) with $C_{\text{Ga-In}}$=72 cm K/W [(a) and (b)] and $C_{\text{As-Sb}}$=95 cm K/W (c) (solid lines). The dashed line in (a) is also calculated from Eq. (2) with a properly chosen value of W_{InN}=0.5 cm K/W (open circle), instead of the ceramics value W_{InN} =2.22 cm K/W (solid line). The solid circles represent the experimental data of the end point binary materials listed in Table I.

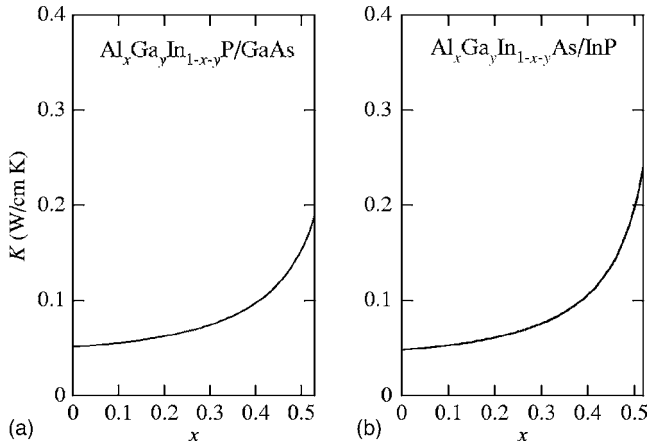

FIG. 12. Thermal conductivity K vs composition x for some III−V quaternary alloys: (a) $Al_xGa_yIn_{1-x-y}P/GaAs$ and (b) $Al_xGa_yIn_{1-x-y}As/InP$. These estimated values are calculated from Eq. (12) with $C_{\text{Al-Ga}}=32$ cm K/W, $C_{\text{Al-In}}=15$ cm K/W, and $C_{\text{Ga-In}}=72$ cm K/W.

$$y = 0.4674 - 0.9800x \quad (0 \le x \le 0.48, 0 \le y \le 0.47), \tag{16}$$

for $Al_xGa_yIn_{1-x-y}As/InP$.

V. CONCLUSIONS

We analyzed the room-temperature thermal conductivity of group-IV and III−V semiconductor alloys using a simplified model of the alloy scattering. The present model requires one disorder parameter ($C_{\alpha-\beta}$) for group-IV binary and III–V ternary alloys and two disorder parameters for III–V quaternary alloys, arising from the effects of alloy scattering. Good agreement is achieved between the present model and published experimental data on various group-IV and III–V semiconductor alloys. Using these analysis results, we obtain an expression, $C_{\alpha-\beta}=(\Gamma/7.7)^{-0.90}$ which enables us to estimate the disorder parameter $C_{\alpha-\beta}$ with optional alloy with the dimensionless scattering strength Γ defined by the difference between the mass of the substitutional atom (α or β) and the average atomic mass. For example, we obtain $C_{\text{Al-In}}=15$ cm K/W used for estimating the lattice thermal conductivity of (Al, In)-based alloys, such as $Al_xIn_{1-x}N$, $Al_xIn_{1-x}As_ySb_{1-y}$, and $Al_xGa_yIn_{1-x-y}N$. An ordering effect is also discussed for the explanation of some intermetallic and semiconductor compounds. The thermal conductivity of 3C-SiC is adequately described by recognizing this material as a perfectly ordered material of C_xSi_{1-x} alloy.

[1] B. Abeles, Phys. Rev. **131**, 1906 (1963).
[2] S. Adachi, J. Appl. Phys. **54**, 1844 (1983).
[3] W. Nakwaski, J. Appl. Phys. **64**, 159 (1988).
[4] L. Nordheim, Ann. Phys. **401**, 607 (1931).
[5] L. Nordheim, Ann. Phys. **401**, 641 (1931).
[6] P. Jacobsson and B. Sundqvist, J. Phys. Chem. Solids **49**, 441 (1988).
[7] A. Mascarenhas, *Spontaneous Ordering in Semiconductor Alloys* (Kluwer Academic, New York, 2002).
[8] T. S. Kuan, T. F. Kuech, W. I. Wang, and E. L. Wilkie, Phys. Rev. Lett. **54**, 201 (1985).
[9] A. Ourmazd and J. C. Bean, Phys. Rev. Lett. **55**, 765 (1985).
[10] M. A. Afromowitz, J. Appl. Phys. **44**, 1292 (1973).
[11] J. L. Pichardo, J. J. Alvarado-Gil, A. Cruz, J. G. Mendoza, and G. Torres, J. Appl. Phys. **87**, 7740 (2000).
[12] S. Adachi, *GaAs and Related Materials: Bulk Semiconducting and Superlattice Properties* (World Scientific, Singapore, 1994).
[13] E. T. Croke, A. T. Hunter, C. C. Ahn, T. Laursen, D. Chandrasekhar, A. E. Bair, D. J. Smith, and J. W. Mayer, J. Cryst. Growth **175–176**, 486 (1997).
[14] S. Adachi, *Properties of Group-IV, III−V, and II−VI Semiconductors* (Wiley, Chichester, 2005).
[15] M. Asheghi, K. Kurabayashi, R. Kasnavi, and K. E. Goodson, J. Appl. Phys. **91**, 5079 (2002).
[16] D. G. Cahill and F. Watanabe, Phys. Rev. B **70**, 235322 (2004).
[17] T. R. Anthony, W. F. Banholzer, J. F. Fleischer, L. Wei, P. K. Kuo, R. L. Thomas, and R. W. Pryor, Phys. Rev. B **42**, 1104 (1990).
[18] D. G. Onn, A. Witek, Y. Z. Wie, T. R. Anthony, and W. F. Banholzer, Phys. Rev. Lett. **68**, 2806 (1992).
[19] J. R. Olson, R. O. Pohl, J. W. Vandersande, A. Zoltan, T. R. Anthony, and W. F. Banholzer, Phys. Rev. B **47**, 14850 (1993).
[20] W. S. Capinski, H. J. Maris, E. Bauser, I. Silier, M. Asen-Palmer, T. Ruf, M. Cardona, and E. Gmelin, Appl. Phys. Lett. **71**, 2109 (1997).
[21] J. P. Dismukes, L. Ekstrom, E. F. Steigmeier, I. Kudman, and D. S. Beers, J. Appl. Phys. **35**, 2899 (1964).
[22] C. B. Vining, W. Laskow, J. O. Hanson, R. R. Van der Beck, and P. D. Gorsuch, J. Appl. Phys. **69**, 4333 (1991).
[23] B. C. Daly, H. J. Maris, A. V. Nurmikko, M. Kuball, and J. Han, J. Appl. Phys. **92**, 3820 (2002).
[24] W. Liu and A. A. Balandin, Appl. Phys. Lett. **85**, 5230 (2004).
[25] G. A. Slack and S. B. Austerman, J. Appl. Phys. **42**, 4713 (1971).
[26] M. S. Abrahams, R. Braunstein, and F. D. Rosi, J. Phys. Chem. Solids **10**, 204 (1959).
[27] D. G. Arasly, R. N. Ragimov, and M. I. Aliev, Sov. Phys. Semicond. **24**, 225 (1990).
[28] Y. B. Magomedov, N. L. Kramynina, and S. M. Ismaílov, Sov. Phys. Solid State **34**, 1486 (1992).
[29] M. C. Ohmer, W. C. Mitchel, G. A. Graves, D. E. Holmes, H. Kuwamoto, and P. W. Yu, J. Appl. Phys. **64**, 2775 (1988).
[30] F. Szmulowicz, F. L. Madarasz, P. G. Klemens, and J. Diller, J. Appl. Phys. **66**, 252 (1989).
[31] T. Borca-Tasciuc, D. W. Song, J. R. Meyer, I. Vurgaftman, M.-J. Yang, B. Z. Nosho, L. J. Whitman, H. Lee, R. U. Martinelli, G. W. Turner, M. J. Manfra, and G. Chen, J. Appl. Phys. **92**, 4994 (2002).
[32] R. O. Carlson, G. A. Slack, and S. J. Silverman, J. Appl. Phys. **36**, 505 (1965).
[33] P. D. Maycock, Solid-State Electron. **10**, 161 (1967).
[34] R. Bowers, J. E. Bauerle, and A. J. Cornish, J. Appl. Phys. **30**, 1050 (1959).
[35] W. Both, A. E. Bochkarev, A. E. Drakin, and B. N. Sverdlov, Cryst. Res. Technol. **24**, K161 (1989).
[36] W. Both, V. Gottschalch, and G. Wagner, Cryst. Res. Technol. **21**, K85 (1986).